ACOUSTIC ATTENUATION OF SIDE BRANCH RESONATORS APPLIED IN DUCT SYSTEM

Paulo Henrique Mareze, paulo@lva.ufsc.br
Arcanjo Lenzi, arcanjo@lva.ufsc.br
LVA – Laboratory of Vibration and Acoustics – Federal University of Santa Catarina – 88040-900 – Florianópolis/SC – Brazil.

Abstract. *The side branch resonators, which produces a narrow band of high acoustic attenuation at regularly spaced frequency intervals, is a common type of silencer used in ducts. The present work considers T shaped acoustic resonator applied in duct systems. The motivation of the study is associated with the noise attenuation systems of reciprocating compressors that employ side branch acoustic resonators. Numerical simulations, based in a linear acoustic approach for a three-dimensional acoustic resonator are compared to acoustical measurements and the analytical model.*

Keywords*: Side branches, acoustic filters, visco-thermal wave propagation.*

1. INTRODUCTION

Side branch resonators are acoustic reactive elements of sound absorption, tunable to multiple or specific frequencies. These resonators can be applied to noise control in ducts or acoustic filters, for example mufflers of compressors. The sound attenuation of reactive absorbers is usually provided by abrupt changes in acoustic impedance, with the coupling of acoustic geometries. The losses by viscous and thermal effects inside the ducts are an important factor in sound absorption, which should to be taken into account. To understand the characteristics of the side branches sound attenuation in ducts, a search through experimental procedures, analytical and computational models have done in this work. Aiming to optimize the attenuation of resonant tubes, were applied to the optimization methods of analytical models of ducts in relation to the parameters of design and implementation.

The analytical model through linear acoustics provides only the longitudinal modes of the tubes, which is validated numerically and experimentally for frequencies below the cut-off. These models were compared by assessments made from the response function in frequency, which represents the ratio between the sound pressures measured at the entrance and exit of the geometry considered. Inside tubes of small diameter the wave propagation is affected by viscosity and thermal conductivity of the fluid. This visco-thermal effect has been considered on the analytical and numerical models. Some considerations are taking for this analytical model. Among them, it is the fluid stationary, not the internal generation of heat, linear acoustic behavior (small-amplitude waves), whereas large wave length compared to the radius of the tube.

The motivation of the study is associated with the noise attenuation systems of reciprocating compressors that employ side branch acoustic resonators applied in ducts. Numerical simulations, based in a linear acoustic approach for a three-dimensional acoustic resonator are compared to acoustical measurements and the analytical model. To allow a detailed analysis of the flow effects over the acoustic system, experimental measurements of a duct system with flow and acoustic resonator applied are performed.

2. ANALYTICAL MODEL

The application of a side branch in a main duct, shown in Figure 1, presents the following variables, where P_A and P_B are complex constants and represent the incident and reflected waves before the application of the resonant tube, P_C and P_D represent the incident and reflected waves after the application of the resonant tube. The incident and reflected waves inside the duct are P_E and P_F, respectively. The boundary conditions are unit pressure at the entrance and radiation impedance at end of the main duct. The main duct present cross-sectional area S_1, length $L_T = L_1 + L_2$ and impedance and radiation Z_1. The resonant tube present cross-sectional area S_2, length L_r and impedance of radiation for open tube or a closed tube (wall rigid particle with zero particle velocity). The excitation of pressure ($P_o e^{-jwt}$) is applied at the entrance of the main duct, and P_o=1 for instance. The schematic of the analytical model is shown in the Figure 1.

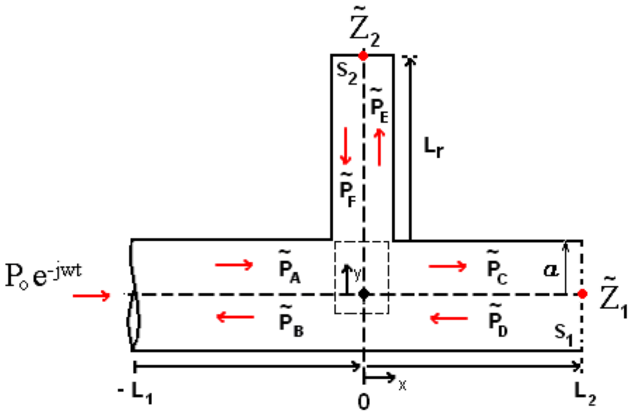

Figure 1 - Analytical model.

There is an independent coordinate system for the pressure field inside the resonator, which is given by:

$$\tilde{P} = \begin{cases} \tilde{P}_1(x,t) = (\tilde{P}_A e^{jkx} + \tilde{P}_B e^{-jkx})e^{-jwt} & \text{-L}_1 < x < 0 \\ \tilde{P}_2(x,t) = (\tilde{P}_C e^{jkx} + \tilde{P}_D e^{-jkx})e^{-jwt} & 0 < x < \text{L}_2 \\ \tilde{P}_3(y,t) = (\tilde{P}_E e^{jky} + \tilde{P}_F e^{-jky})e^{-jwt} & 0 < y < \text{L}_r \end{cases} \tag{1}$$

At the entrance of the main duct, there is the following boundary condition:

$$P(-L_1, t) = P_o e^{-jwt} \tag{2}$$

where w is the angular frequency. For more about duct acoustics and mufflers see Munjal (*1*).

The boundary condition is not zero at the open end, because the open end of the duct radiates sound into the surrounding medium. The proper value for the terminating impedance is the radiation impedance of the open end of the pipe. The radiation impedance is complex; the real part (radiation resistance) represents the energy radiated away from the open end in the form of sound waves, and the imaginary part (radiation reactance) represents the mass loading of the air just outside the open end.

Therefore, the boundary conditions at the end based on the acoustic radiation impedance of a tube (constant circular cross section) with non-flanged open end, which according to Pierce (*2*) is given by Equation (3) (ka <<1).

$$\tilde{Z}_1(L_2, t) = \frac{P(L_2,t)}{u(L_2,t)} = \frac{\rho_o c_o}{S}\left[\frac{1}{4}(ka)^2 + j0.61(ka)\right] \tag{3}$$

where $\rho_o c_o$ is the characteristic impedance of the gas, k is the wave number , a is the radius of the main duct and $S=\pi a^2$ is the area. For flanged open ends, the radiation impedance is:

$$\tilde{Z}_1(L_2, t) = \frac{\rho_o c_o}{S}\left[\frac{1}{2}(ka)^2 + j\frac{8}{3\pi}(ka)\right] \tag{4}$$

For an open-end resonator, $\tilde{Z}_2$ gives the same equation (3) dependent of the resonator radio. For a closed-end resonator we have $u(L_r, t) = 0$ and $\tilde{Z}_2$ tend to infinity. The effective length of the non-flanged mean duct is $L_T + 0.61a$.

A general model for the calculation of resonant frequencies of long T-shaped acoustic resonator has been derived by Vipperman (*3*), providing by the plane wave assumption like this case. Solving the equations of continuity and energy for an ideal gas is obtained a system of six equations and six unknowns for the case with one side branch, which is resolved in the frequency domain, given by:

$$\text{Continuity of pressure}\quad \begin{cases} \tilde{P}_A e^{-jkL_1} + \tilde{P}_B e^{jkL_1} = P_0; \\ \tilde{P}_A + \tilde{P}_B - \tilde{P}_C - \tilde{P}_D = 0; \\ \tilde{P}_C + \tilde{P}_D - \tilde{P}_E - \tilde{P}_F = 0; \end{cases} \qquad (x = 0)$$

$$\text{Mass conservation}\quad \left\{ \rho_0 \left[s_1\tilde{P}_A - s_1\tilde{P}_B - s_1\tilde{P}_C + s_1\tilde{P}_D - s_2\tilde{P}_E + s_2\tilde{P}_F \right] = 0; \quad (x = 0) \right.$$

$$\text{Impedance condition}\quad \begin{cases} \tilde{P}_C \left[1 - \dfrac{\tilde{Z}_1}{\rho_0 c_0}\right] e^{jkL_2} + \tilde{P}_D \left[1 + \dfrac{\tilde{Z}_1}{\rho_0 c_0}\right] e^{-jkL_2} = 0; & (x = L_2) \\ \tilde{P}_E \left[1 - \dfrac{\tilde{Z}_2}{\rho_0 c_0}\right] e^{jkL_r} + \tilde{P}_F \left[1 + \dfrac{\tilde{Z}_2}{\rho_0 c_0}\right] e^{-jkL_r} = 0; & (y = L_r) \end{cases}$$

Writing these equations in the matrix form:

$$\begin{bmatrix} e^{-jkL_1} & e^{jkL_1} & 0 & 0 & 0 & 0 \\ 1 & 1 & -1 & -1 & 0 & 0 \\ 0 & 0 & 1 & 1 & -1 & -1 \\ s_1 & -s_1 & -s_1 & s_1 & -s_2 & s_2 \\ 0 & 0 & \left[1 - \dfrac{\tilde{Z}_1}{\rho_0 c_0}\right] e^{jkL_2} & \left[1 + \dfrac{\tilde{Z}_1}{\rho_0 c_0}\right] e^{-jkL_2} & 0 & 0 \\ 0 & 0 & 0 & 0 & \left[1 - \dfrac{\tilde{Z}_2}{\rho_0 c_0}\right] e^{jkL_r} & \left[1 + \dfrac{\tilde{Z}_2}{\rho_0 c_0}\right] e^{-jkL_r} \end{bmatrix} \begin{bmatrix} \tilde{P}_A \\ \tilde{P}_B \\ \tilde{P}_C \\ \tilde{P}_D \\ \tilde{P}_E \\ \tilde{P}_F \end{bmatrix} = \begin{bmatrix} P_0 \\ 0 \\ 0 \\ 0 \\ 0 \\ 0 \end{bmatrix} \qquad (5)$$

Solving this system, we can find the variables P_A to P_F in the frequency domain. The response function is the logarithm of the acoustic pressure ratio at the end and at the entrance of the main duct in decibels.

$$\begin{gathered} H(f) = 20Log\left(\left| \frac{\tilde{P}_3(L_2, f)}{\tilde{P}_1(-L_1, f)} \right| \right) \\ H(f) = 20Log\left(\left| \frac{\tilde{P}_C e^{jL_2 2\pi f / c_o} + \tilde{P}_D e^{jL_2 2\pi f / c_o}}{\tilde{P}_A e^{-jL_1 2\pi f / c_o} + \tilde{P}_B e^{jL_1 2\pi f / c_o}} \right| \right) \end{gathered} \qquad (6)$$

Another kind of passive silencers like Helmholtz resonators and perforated plates can be applied in ducts, according Beranek (*4*) and Kinsler (*5*). To attenuate noise in small enclosures, applied resonators are tuned in multiple or specific frequencies reducing the acoustic radiated power from the cavity, observed in Li (*6*) and Park (*7*). Ingard (*8*) discuss some properties of a resonator in a free field or in a wall in regard to scattering and absorption of an incident plane wave.

The response function can be minimized applying genetic algorithm (GA) to the analytical model optimizing the parameters or variables, related to length, diameter, positioning on the main duct and numbers of side branches applied. For an overview about genetic algorithm see Goldberg (*9*). Using some *Matlab GA tools*, this analytical optimization can be simple and useful for this kind of problem. For this case was used a population of 300 individuals and one per cent of mutation. The objective function that needs to minimize is the global value of the transfer function, calculated in one-third octave. The stop criterion adopted was 7dB of reduction in this overall value. Applying this optimization we find four optimized closed-end resonators on a main duct of length 48.25*mm* and radius 3.2*mm*, and 7 dB of global attenuation was obtained. The resonators have a radius of 1.6*mm* and lengths of respectively 26.85*mm*, 21.00*mm*, 15.60*mm*, 10.03*mm*. The positions measured from entry are respectively 22.9*mm*, 24.12*mm*, 30*mm* and 36.19*mm*. The results of numerical and experimental model will be compared.

3. VISCOTHERMAL EFFECTS

Sound propagation in prismatic tubes has been investigated thoroughly by many authors. For an overview see Eerden (*10, 11*) and Beltman (*12*). In this paper the low reduced frequency solution, which includes viscous and thermal effects, is used to describe the acoustic behavior of gas inside branch resonators. For a prismatic tube with rigid walls the low reduced frequency model has the following one-dimensional solution for the pressure perturbation P and the velocity perturbation u:

$$\begin{aligned} P(x,t) &= \left[\tilde{P}_A e^{\Gamma kx} + \tilde{P}_B e^{-\Gamma kx}\right] e^{-\Gamma wt} \\ u(x,t) &= \frac{G}{\rho_0 c_0}\left[\tilde{P}_A e^{\Gamma kx} - \tilde{P}_B e^{-\Gamma kx}\right] e^{-\Gamma wt} \end{aligned} \tag{7}$$

An important parameter is the viscothermal wave propagation coefficient Γ. It is a complex quantity, where $c_o / \mathrm{Im}[\Gamma]$ represents the phase velocity and $\mathrm{Re}[\Gamma]$ accounts for the attenuation of a propagating wave. It is noted that Γ is frequency dependent and a function of the shear wave number $s = a\sqrt{\rho_0 w / \mu_0}$ and the square root of the Prandtl number σ, where μ_0 is the gas viscosity.

The shear wave number is a measure for the ratio of inertial and viscous forces and can be seen as an acoustic Reynolds number. For a low shear wave number the viscous effects dominate and the velocity perturbation in the tube approaches a Poiseuille flow. For a high value of s an almost plane wave front results. The factor G depends of the geometric characteristic of the duct, and the coefficient propagation for a narrow and wide cylindrical duct is:

$$\Gamma = \sqrt{\frac{J_0(j\sqrt{j}s)}{J_2(j\sqrt{j}s)}\frac{\gamma}{n}} \tag{8}$$

where n is a polytropic coefficient which characterizes the thermodynamically process within the tube. The terms J_0 is and J_2 are the zero and second order Bessel functions, and γ is the ratio of specific heats.

$$n = \left(1 + \frac{\gamma - 1}{\gamma}\frac{J_2(j\sqrt{j}s\sigma)}{J_0(j\sqrt{j}s\sigma)}\right)^{-1} \tag{9}$$

In this case, the coefficient G is:

$$G = -\frac{j}{\Gamma}\left(\frac{\gamma}{n}\right) \tag{10}$$

For numerical models, we can represent this visco-thermal effect through the complex sound propagation $\tilde{c}$, where is a new coefficient frequency dependent and a function of Γ. If we consider a complex wave number $\tilde{k}$, where

$$\begin{aligned} \tilde{k} &= \frac{\Gamma\, k}{j} \\ \frac{w}{\tilde{c}} &= \frac{\Gamma w}{j c_0} \end{aligned} \tag{11}$$

is possible to write the complex sound propagation:

$$\tilde{c} = \frac{j\, c_0}{\Gamma} \tag{12}$$

where the real part represents the phase velocity and the imaginary part represents the attenuation. This complex sound propagation depends on the diameter of the duct related to shear wave number, according Figure 2.

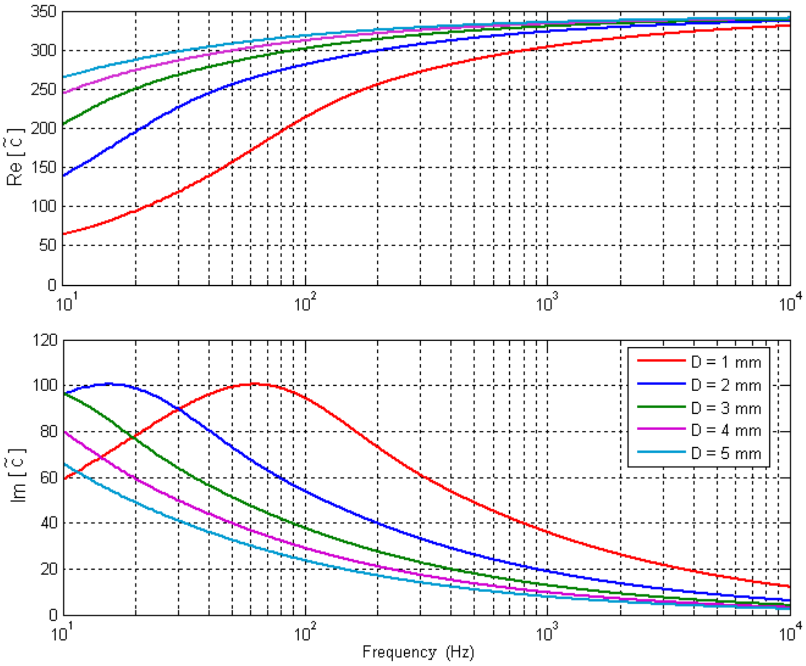

Figure 2 - Complex sound propagation $\tilde{c}$ function of diameter *D* of the duct, air at 20ºC.

So, this complex velocity of the sound will represent the visco-thermal effect on the numerical model, to validate the experiments and the analytical model.

4. NUMERICAL MODEL

The objective of the numerical simulation is obtaining a discretized domain with small elements and calculate the acoustic velocities and pressures at all nodes of the mesh geometry, representing the fluid inside the tubes. For the solution we need to apply properties for that make up the field and the conditions set out in the boundary contour problem. In this work the FEM method (Finite Element Method) has been used through the *Virtual Lab* software and is performed in the frequency domain in steady state. The calculation of the response function has been obtained by solving the pressure field. The mesh of the optimized geometry and boundary conditions of unit pressure at the entrance and radiation admittance is shown in Figure 3, where admittance is the inverse of impedance.

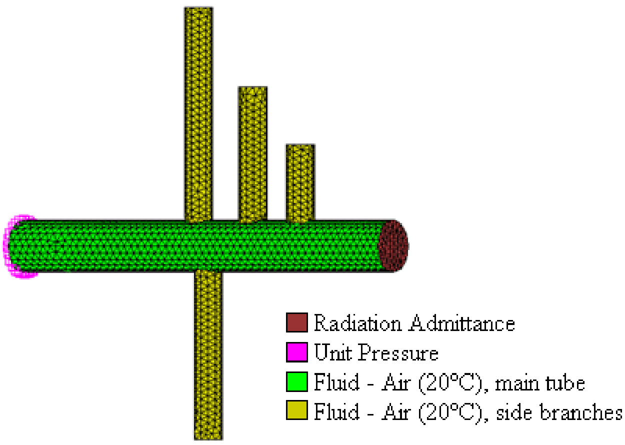

Figure 3 - The mesh of the optimized geometry and boundary conditions.

The visco-thermal effects in a duct basically depend on the diameter of the duct, the frequency and the properties of the gas. This visco-thermal effect was applied in the numerical model through the complex sound propagation $\tilde{c}$, obtained from the analytical model, according to the diameter of the main duct and resonators ducts.

For this simulation, air is considered at 20ºC ($c_0 = 343,2\ [m/s]$, $\rho_0 = 1,21\ [kg/m^3]$) as the fluid inside the tubes. The mesh is made with discretization of 10 elements per wavelength at the maximum frequency of analysis, where the maximum referred frequency is 10 kHz. The optimized geometry of the mesh gives 25.542 tetrahedrons elements.

4. EXPERIMENTAL MODEL AND RESULTS

The experimental validation was performed with a laboratory test, without flow inside the resonator. The signal analyzer sends a sweeped sine signal to the amplifier and the speaker, generating noise in broad frequency band. The measurement of acoustic pressure is made by two free field microphones B&K 4189, one at the entrance and one at the end of the resonator. The signal of the microphones are sent to the signal analyzer to resolve the transfer function, given by:

$$H(f) = 20Log\left(\left|\frac{p_{mic2}}{p_{mic1}}\right|\right) \tag{13}$$

In Figure 4 the experimental setup is shown.

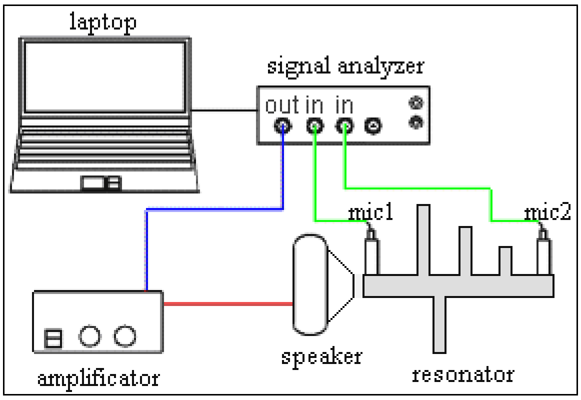

Figure 4 - Experimental apparatus.

The coherence is determined, which is a measure of the correlation between the phases in different points of a wave and is directly related to the characteristics of the source of the wave. It is known that a good measurement gives coherence near 1.0. The measured coherence is shown in Figure 5.

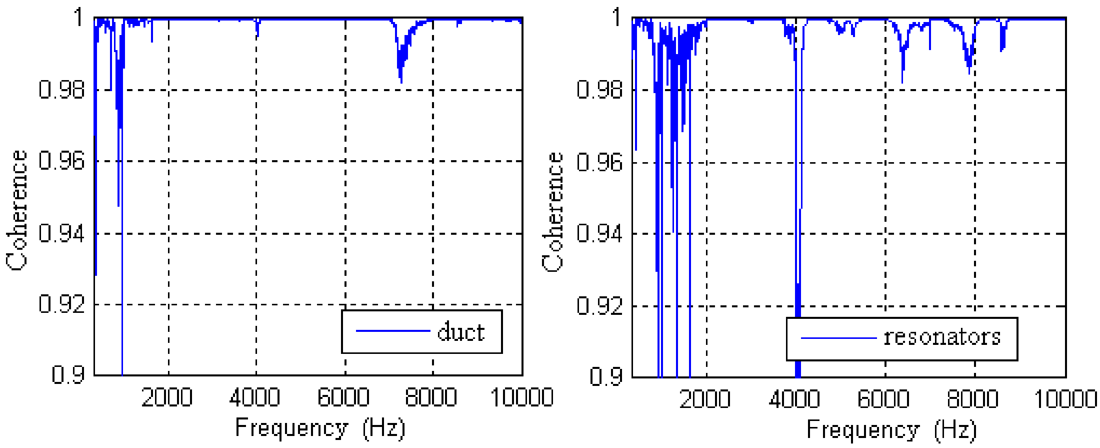

Figure 5 - Experimental coherence.

For the resonators in Figure 5, the reducing coherence at around 4kHz probably accurs due the abrupt decay of the output pressure and loss of signal at the end of the duct. However, this indicates a good quality of the measurement, thus giving consistency to the experimental results. The results are compared with numerical and analytical model in Figure 6.

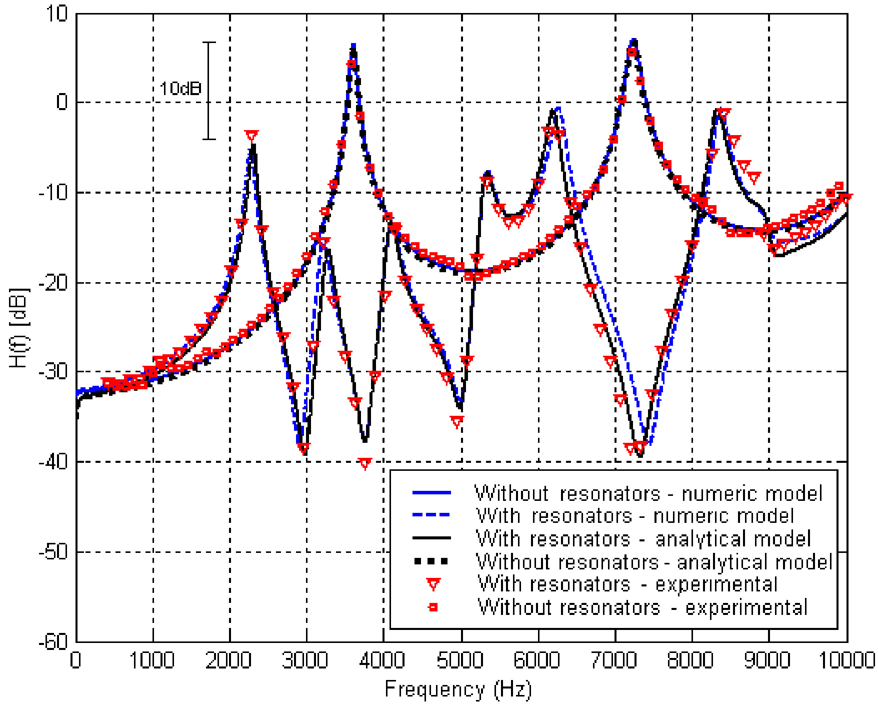

Figure 6 - Comparison of the Response Function.

There is wide agreement of results, validating the used methods, for the case there is no flow. At 7kHz we note some almost agreement due to numerical errors and geometric tolerances in the experimental model. There was obtained an attenuation of 10 dB for the first mode of the main duct shown in Figure 5. The global attenuation obtained by one-third octave frequency is 7 dB.

5. CONCLUSIONS

High correlation was observed between the analytical, numerical model and experimental analysis, validating these tools of analysis of sound absorption for side branch resonator. The visco-thermal model was applied efficiently to the analytical and numerical model, correcting the amplitude of the resonances according the experimental method. The genetic algorithm was implemented successfully at the analytical model reducing the global response function associated with the duct. The effectiveness application of the a quarter wavelength resonator depends strongly on the location at the main duct and they can be tuned by varying the geometry. If the resonator is connected to the main duct at a position near an anti-node of its modes the original mode split and the attenuation are large; moreover, resonator damping increases the total damping of the system.

It's possible to apply other kinds of resonators at ducts or cavities and optimize the configuration to minimize the sound power radiated from the system.

6. ACKNOWLEDGEMENTS

The authors would like to acknowledge the financial support by CAPES.

7. REFERENCES

[1] M. L. Munjal, "*Acoustics of ducts and mufflers with applications to exhaust and ventilation system"*, Interscience, NewYork (1987).

[2] A.D. Pierce, "*Acoustics: An Introduction to Its Physical Principles and Applications*", Acoustical Society of America, New York, 1989.

[3] J. S. Vipperman and D. Li, "*On the design of long T-shaped acoustic resonators*", J. Acoust. Soc. Am. 116, 2785–2792 , 2004.

[4] Leo L. Beranek and István L. Vér. "*Noise and Vibration control Engineering: Principles and applications*". John Wiley, New York, 1992.

[5] L. E. Kinsler, A. R. Frey, A. B. Coppens, and J. V. Sanders, "*Fundamentals of Acoustics*", 4th ed. Wiley, New York, 2000.

[6] D. Li and J. S. Vipperman, "*Noise control in enclosures: Modeling and experiments with T-shaped acoustic resonators",* J. Acoust. Soc. Am. vol. 122, issue 5, p. 2615, 2007.

[7] Park, Ju Hyun; Sohn, Hoon, "*On optimal design of half-wave resonators for acoustic damping in an enclosure",* J. Acoust. Soc. Am. Volume 319, Issue 3-5, p. 807-821., 2008.

[8] K.U. Ingard, "*On the theory and design of acoustic resonators*", Journal of the Acoustical Society of America 25 1037–1061, 1953.

[9] Goldberg, D. E. "*Genetic Algorithms in Search, Optimization and Machine Learning*", 1989, Cambridge, Addison-Wesley.

[10] Eerden, Frits Van Der, "*Reduction with coupled prismatic tubes"*, PhD thesis, University of Twente, Enschede, The Netherlands, 2000.

[11] Eerden, Frits Van Der, F.J.M. and Tijdeman, H. "*Acoustic impedance of coupled tubes including visco-thermal effects".* In: The 1999 Congress and Exposition on Noise Control Engineering, Inter-Noise '99, 6-8 December 1999, Fort Lauderdale, USA.

[12] Beltman, W.M. (1999a), "*Visco-thermal wave propagation including acousto-elastic interaction, part I: theory*", Journal of Sound and Vibration 227(3), 555-586.

8. RESPONSIBILITY NOTICE

The author(s) is (are) the only responsible for material included in this paper.